福井大学リポジトリ
UFR
UNIVERSITY OF FUKUI REPOSITORY

Evaluation of the Initial Stage of Formation of Ti/Al Ohmic Contacts Using Photoresponse Method

メタデータ	言語: eng
	出版者:
	公開日: 2013-07-04
	キーワード (Ja):
	キーワード (En):
	作成者: Shiojima, Kenji, Yokohama, Hideo, Araki, Gako
	メールアドレス:
	所属:
URL	http://hdl.handle.net/10098/7600

(C)公益社団法人応用物理学会 2013/ 2013 The Japan Society of Applied Physics

Evaluation of the Initial Stage of Formation of Ti/Al Ohmic Contacts Using Photoresponse Method

Kenji Shiojima[1], Hideo Yokohama[1, 2], and Gako Araki[2]

[1]Graduate School of Electrical and Electronics Engineering, University of Fukui, Fukui 910-8507, Japan

[2] Optorans, Kawasaki 214-0014, Japan

Ti/Al contacts formed on n-GaN and AlGaN/GaN layers upon annealing at temperatures below the melting point of Al were evaluated by photoresponse (PR), current-voltage (I-V), and secondary ion mass spectroscopy (SIMS) measurements. In the PR spectra, the photocurrent based on the internal photoemission was detected, and the Schottky barrier height ($q\phi_B$) was determined for all the samples, even though the I-V characteristics were very leaky. The AlGaN/GaN samples had constant $q\phi_B$ values of 0.85-1.0 eV independent of the annealing temperature. In contrast, the n-GaN samples had very low $q\phi_B$ values of 0.2 eV under the as-deposited condition. Upon annealing, $q\phi_B$ significantly increases and finally reaches almost the same values as those of the AlGaN/GaN samples. This can be explained by the change from Ti- to Al-rich interfaces in conjunction with the SIMS results.

1. Introduction

Ti/Al-based ohmic contacts have been widely used with n-GaN layers and AlGaN/GaN high-electron-mobility transistor (HEMTs) structures. For practical use, cap layers typically consisting of a refractory metal and Au are formed on the Ti/Al contacts in order to avoid dissolving the Al layer in the development solution, improve the contact with interconnection layers, and prevent the interfacial reaction between Al and Au.[1) However, the most important role of the low contact resistance (R_C) is in metal (Ti/Al)/semiconductor (GaN, AlGaN) interfaces. Many studies have been reported on fabricating improved Ti/Al-based ohmic contacts from the aspects of surface treatments, the metal deposition technique, the metal-layer-thickness dependence, and annealing conditions.[2-16)] Typical ways evaluating Ti/Al contacts are measurements of R_C by the transmission line method after annealing with one of the process conditions changed as a parameter. Also, the interfacial reaction has been observed by transmission electron microscopy and secondary ion mass spectroscopy (SIMS).[17)] As a result of these works, some ohmic formation mechanisms has been reported such as the formation of TiN and N-vacancies, and the removal of a native oxide layer by Ti, resulting in the formation of Al/clean GaN interfaces.[18)] The reported annealing temperatures were in a wide range and can be classified into three ranges. Above the melting point of Al (660 °C), 800-900 °C, the contacts reacted completely.[2, 3)] Around the melting point, the reaction occurred in the vicinity of the interface.[19)] At temperatures much lower than the melting point, 400 °C, with a long annealing time, ohmic contacts can be formed.[20, 21)] Additionally, crystal quality of GaN and AlGaN affects R_C. In particular, AlGaN layers on GaN contain surface defects and residual donors. Since these factors have improved with the progress of epitaxial growth techniques, the reestablishment of an ohmic formation technique is often required.[22)]

There is a wide variation in the reported results for single-metal-layer contacts with n-GaN. Originally leaky current-voltage (I-V) characteristics for Ti and Al contacts were reported by Schmitz et al.[23)] On the other hand, the Schottky barrier heights ($q\phi_B$) of Ti contacts were reported to be 0.20, 0.58, and 0.60 eV by I-V measurements.[24-26)] Relatively high $q\phi_B$ values of 0.60 and 0.8 eV were obtained for

Al contacts by I-V and X-ray photoemission spectroscopy measurements, respectively.[27)]

Although many efforts have been made to obtain lower R_C through Ti/Al-based metallization, understanding of the formation mechanism of ohmic contacts remains elusive owing to the complicated interface condition. In this paper, we focus on evaluating Ti/Al contacts formed on both n-GaN and AlGaN/GaN HEMT structures annealed at temperatures of up to the ohmic formation temperature. We mainly used the photoresponse (PR) method, which can be used even for leaky contacts, to determine $q\phi_B$.

2. Experimental Procedure

Figure 1 shows the sample structure used in this study. Both a 2-μm-thick Si-doped n-GaN single layer ($N_D = 1\times10^{17}$ cm^{-3}) and AlGaN (15 and 21 nm thick)/GaN (2 μm thick) HEMT structures were grown on c-plane sapphire substrates by metalorganic chemical vapor deposition (MOCVD). The Al content in the AlGaN layers was 25%. The measured sheet resistance and electron mobility were 561 and 507 Ω/sq, and 1776 and 1660 cm^{2}V^{-1}s^{-1}, for the HEMT wafers with AlGaN thicknesses of 15 and 21 nm, respectively.

Firstly, large-area Ti (20 nm thick)/Al (200 nm thick) electrodes were deposited by electron-beam evaporation, and annealed at 700 °C for 30 s to form practical ohmic contacts. Then, Ti (20 nm thick)/Al (200 nm thick) dots (200 μmϕ) were deposited as evaluation contacts. Surface treatment before the metal deposition was conducted with buffered hydrofluoric acid solution. Finally, rapid isothermal annealing for 30 s was conducted in N_2 atmosphere. The typical distance between the practical and evaluation contacts was about 1 mm.

In the PR measurements, when monochromatic light with a photon energy (hν) greater than $q\phi_B$ is incident on a metal/GaN interface, carriers in the metal can surmount the Schottky barrier and a photocurrent may be generated, which is called the internal photoemission effect. The $q\phi_B$ can be determined from the measured photoemission using Fowler's equation: [28)]

$$Y^{\frac{1}{2}} \propto \left(h\nu - q\phi_B\right), \qquad (1)$$

where Y is the measured photoemission yield. When hν is close to the band edge, owing to the generation of electron-hole pairs, a large photocurrent flows similarly to in a solar cell.

I-V measurements were also conducted with an HP 4142B semiconductor parameter analyzer. The interfacial reaction was characterized by SIMS measurements with an ULVAC PHI ADEPT 1010 system. A Cs^+-ion beam was used as a primary ion source to detect Ga, Ti, and Al ions at 1 keV. The beam raster size was 500×500 μm^2.

3. Results

3.1 I-V characteristics

Figures 2(a) and 2(b) show typical forward I-V characteristics of the Ti/Al contacts on n-GaN and 15-nm-thick AlGaN/GaN layers under the as-deposited condition and after annealing at temperatures of up to 600 °C in a linear plot, respectively. The I-V characteristics of the contacts on a 21-nm-thick AlGaN layer are basically the same as those on a 15-nm-thick AlGaN layer. When the annealing temperature is up to 500 °C for n-GaN and 520 °C for AlGaN/GaN samples, the I-V curves show leaky Schottky or ohmic characteristics. Since there is no linear region in the forward I-V curves in a semi-log plot, $q\phi_B$ cannot be determined. When the annealing temperature is above these values, the characteristics become ohmic.

Figure 3 shows the annealing temperature dependence of the reverse biased current at V = -2 V for all the samples. For the n-GaN samples, the reverse current decreases by two orders of magnitude as the annealing temperature increases to 500 °C. When the contacts become ohmic at a higher annealing temperature, the current greatly increases to 30 mA. On the other hand, for AlGaN/GaN samples, upon annealing up to 520 °C, the current is virtually constant at approximately 2 mA. When the contacts become ohmic, the current also increases. The current, however, is smaller than that of n-GaN, because the sheet resistance of the n-GaN sample is smaller than that of the HEMT samples.

3.2 PR spectra

Figure 4 shows the PR spectra of the (a) n-GaN and (b) 15-nm-thick AlGaN/GaN

samples in a wide energy range. The PR spectra for the 21-nm-thick AlGaN/GaN samples are not shown in this paper, but they are the same as those for the 15-nm-thick AlGaN samples. For the n-GaN samples annealed at temperatures of up to 500 °C, large peaks of fundamental absorption near the energy band gap (E_g) of GaN are seen. On the lower side of the peaks, the PR spectrum shows good linearity against $Y^{1/2}$; thus the photocurrent is considered to be based on the internal photoemission according to Fowler's equation. After annealing at above 500 °C, the PR signal intensity significantly decreases. In particular, on the lower side of E_g, no effective signal was detected, thus $q\phi_B$ was not determined. For the AlGaN/GaN samples, the same trend is observed on the lower side. However, the PR signals drop at approximately E_g, because light is absorbed in the GaN layer and the generated carriers cannot reach the metal/AlGaN interface. After annealing at above 520 °C, the fundamental absorption peaks can be seen.

Figure 5 shows a summary of the $q\phi_B$ values obtained from the PR measurements. The 15-nm-thick AlGaN/GaN samples show constant $q\phi_B$ values of approximately 0.85 eV independent of the annealing temperature. The 21-nm-thick samples have a slightly higher $q\phi_B$ value of 1.0 eV under the as-deposited condition. Then, $q\phi_B$ gradually decreased to 0.8 eV as the annealing temperature increased. In contrast, the n-GaN samples have very low $q\phi_B$ values of 0.2 eV under the as-deposited condition. Upon annealing, $q\phi_B$ significantly increases and finally reaches almost the same values as those of the AlGaN/GaN samples. This trend is consistent with that of the reverse current as shown in Fig. 3.

3.3 SIMS analysis

Figure 6 shows SIMS depth profiles for Ga, Ti, and Al of the (a) n-GaN and (b) 15-nm-thick AlGaN/GaN samples before and after annealing at 500 °C. Under the as-deposited condition, each signal has the depth profile expected from the device structure. During the annealing, the intensive diffusion of Al atoms through the Ti layer is observed, and these atoms reach the metal/semiconductor and AlGaN/GaN interfaces.

4. Discussion

Firstly, the electrical characteristics of the Ti/Al contacts upon annealing at a lower temperature are discussed. The I-V characteristics were very leaky for both n-GaN and AlGaN/GaN samples. In particular, AlGaN/GaN samples showed very leaky I-V characteristics, because the crystal quality of the AlGaN layers is not as good as that of GaN, and the two-dimensional electron gas channels are close to the contacts. On the other hand, PR measurements successfully revealed $q\phi_B$ values. From the viewpoint of the evaluation technique, this is advantageous for quantitatively characterizing the effects of process conditions, such as surface treatments, metal deposition, metal layer thickness, and annealing, on $q\phi_B$ values.

Next, there was a large difference between the n-GaN and AlGaN/GaN samples in the annealing temperature dependence of $q\phi_B$. For the n-GaN samples, the annealing temperature dependence of $q\phi_B$ can be explained by the change from Ti to Al contacts evaluated by the SIMS results. Additionally, our $q\phi_B$ values obtained by PR of 0.2 eV under the as-deposited condition and 0.75 eV after annealing at 500 °C are in good agreement with reported values for Ti and Al contacts obtained by I-V and X-ray photoemission measurements.[24, 27] Of course, the same migration occurred in the AlGaN/GaN samples, but they showed strong surface Fermi level pinning. As our samples were grown by MOCVD, the AlGaN surfaces have a Ga face and originally contained an Al content of 25%. Such an Al-rich interface might be a candidate for strong pinning and large $q\phi_B$ values before the ohmic formation.

Upon annealing in the higher-temperature range, as a result of the intensive interfacial mixing and reaction, ohmic phase interfaces with low $q\phi_B$ values were formed. The low electrical field at the interface is responsible for the small PR signal. In the AlGaN/GaN samples, the reacted metal formed a direct contact with GaN, and PR peaks appeared around E_g.

Finally, it was confirmed that PR method was useful to characterize the initial stage of formation of Ti/Al ohmic contacts. In further studies, combining the evaluation of electrical characteristics before ohmic sintering and R_C values is expected to clarify the effect of the process conditions and formation mechanism, and reveal better ways of forming ohmic contacts.

5. Conclusions

We reported the evaluation results of Ti/Al contacts formed on n-GaN and AlGaN/GaN layers upon annealing below the melting point of Al by PR, I-V, and SIMS measurements.

In the PR results, the photocurrent based on the internal photoemission was detected and the $q\phi_B$ values were determined, even though the I-V characteristics were very leaky. The AlGaN/GaN samples had constant $q\phi_B$ values of 0.85-1.0 eV independent of the annealing temperature. In contrast, the n-GaN samples had very low $q\phi_B$ values of 0.2 eV under the as-deposited condition. Upon annealing, $q\phi_B$ significantly increases and finally reaches almost the same values as those of the AlGaN/GaN samples. This can be explained by the change from Ti- to Al-rich interfaces in conjunction with the SIMS results.

On the basis of these results, combining the evaluation of electrical characteristics before ohmic sintering and R_C values is expected to clarify the effect of the process conditions and formation mechanism, and reveal better ways of forming ohmic contacts.

Acknowledgment

Part of this work was supported by a Grant-in-Aid for Scientific Research (C) from the Ministry of Education, Culture, Sports, Science and Technology.

References

1) F. M. Mohammed, L. Wang, H. J. Koo, and I. Adesida: J. Appl. Phys. **101** (2007) 033708.

2) M. E. Lin, Z. Ma, F. Y. Huang, Z. F. Fan, L. H. Allen, and H. Morkoç: Appl. Phys. Lett. **64** (1994) 1003.

3) Y. F. Wu, W. N. Jiang, B. P. Keller, S. Keller, D. Kapolnek, S. P. Denbaars, U. K. Mishra, and B. Wilson: Solid-State Electronics **41** (1997) 165.

4) S. Miller and P. Holloway: J. Electron, Mater. **25** (1996) 1709.

5) L. F. Lester, J. M. Brown, J. C. Ramer, L. Zang, S. D. Hersee, and J. C. Zolper: Appl. Phys. Lett. **69** (1996) 2737.

6) D. Qiao, Z. F. Guan, J. Carlton, S. S. Lau, and G. J. Sullivan: Appl. Phys. Lett. **74** (1999) 2652.

7) C.-T. Lee and H.-W. Kao: Appl. Phys. Lett. **76** (2000) 2364.

8) C. F. Lin, H. C. Cheng, G. C. Chi, C. J. Bu, and M. S. Feng: Appl. Phys. Lett. **76** (2000) 1878.

9) Z. Fan, S. N. Mohammad, W. Kim, Ö. Aktas, A. E. Botchkarev, and H. Morkoç: Appl. Phys. Lett. **68** (1996) 1672.

10) H. Amano, M. Koto, K. Hiramatsu, and I. Akasaki: Jpn. J. Appl. Phys. **28** (1989) L2112.

11) S. Nakamura, T. Mukai, and M. Senoh: Jpn. J. Appl. Phys. **30** (1991) L1998.

12) J. S. Foresi and T. D. Moustakas: Appl. Phys. Lett. **62** (1993) 2859.

13) N. Koide, H. Kato, M. Sassa, S. Yamasaki, K. Manabe, M. Hashimoto, H. Amano, K. Hiramatsu, and I. Akasaki: J. Cryst. Growth **115** (1991) 639.

14) P. Hacke, T. Detchprohm, K. Hiramatsu, and N. Sawaki: Appl. Phys. Lett. **63** (1993) 2676.

15) A. Y. C. Yu: Solid-State Electron. **13** (1970) 239.

16) G. S. Mallow and M. B. Das: Solid-State Electron. **25** (1982) 91.

17) B. P. Luther, S. E. Mohney, J. M. Delucca, and R. F. Karlicek, Jr.: J. Electron. Mater. **27** (1998) 196.

18) S. Ruvimov, Z. Liliental-Weber, J. Washburn, K. J. Duxstad, E. E. Haller, Z.-F. Fan, S. N. Mohammad, W. Kim, A. E. Botchkarev, and H. Morkoç: Appl. Phys. Lett. **69** (1996) 1556.

19) K. Kunihiro, K. Kasahara, Y. Takahashi, and Y. Ohno: Jpn. J. Appl. Phys. **39** (2000) 2431.

20) H. J. Lee, S. J. Yu, H. Asahi, S. Ganda, Y. H. Kim, J. K. Rhee, and S. J. Noh: J. Electron. Mater. **27** (1998) 829.

21) B. P. Luther, S. E. Mohney, T. N. Jackson, M. Ashf Khan, Q. Chen, and J. W. Yang: Appl. Phys. Lett. **70** (1997) 57.

22) K. Shiojima, T. Makimura, T. Maruyama, T. Suemitsu, N. Shigekawa, M. Hiroki, and H. Yokoyama: Phys. Status Solidi C **3** (2006) 2360.

23) A. C. Schmitz, A. T. Ping, M. A. Khan, Q. Chen, J. W. Yang, and I. Adesida: J. Electron. Mater. **27** (1998) 255.

24) M. T. Hirsh, K. J. Duxstad, and E. E. Haller: Electron. Lett. **33** (1997) 95.

25) S. C. Binari, H. B. Dietrich, G. Kelner, L. B. Rowland, K. Doverspike, and D. K. Gaskill: Electron. Lett. **30** (1994) 909.

26) L. S. Yu, D. J. Qiao, Q. J. Xing, S. S. Lau, K. S. Boutros, and J. M. Redwing: Appl. Phys. Lett. **73** (1998) 238.

27) C. I. Wu, A. Kahn, A. E. Wickenden, D. Koleske, and R. L. Henry: J. Appl. Phys. **89** (2001) 425.

28) R. H. Fowler: Phys. Rev. **38** (1931) 45.

Figure captions

Fig. 1. (Color online) Device structure of Ti/Al contacts with configuration for PR measurements.

Fig. 2. (Color online) I-V curves of Ti/Al contacts on (a) n-GaN and (b) AlGaN/GaN structures annealed at temperatures of up to 600 °C.

Fig. 3. (Color online) Annealing temperature dependence of the reverse biased current at V = -2 V.

Fig. 4. (Color online) PR spectra for Ti/Al contacts on (a) n-GaN and (b) AlGaN/GaN structures annealed at temperatures of up to 600 °C. Good linearity was observed on the lower side of the band edge, meaning the Schottky barrier height could be obtained.

Fig. 5. (Color online) Schottky barrier height obtained from the PR results as a function of annealing temperature.

Fig. 6. (Color online) SIMS profiles of Ga, Ti, and Al atoms for the (a) n-GaN and (b) AlGaN/GaN samples before and after annealing at 500 °C.

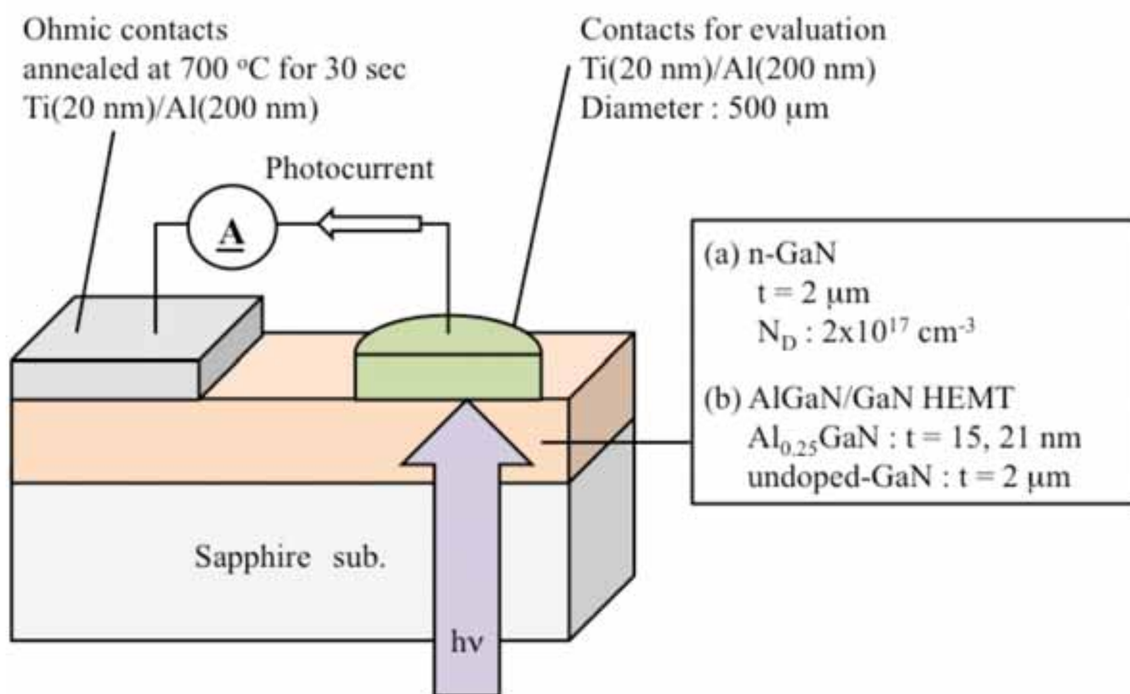

Fig. 1

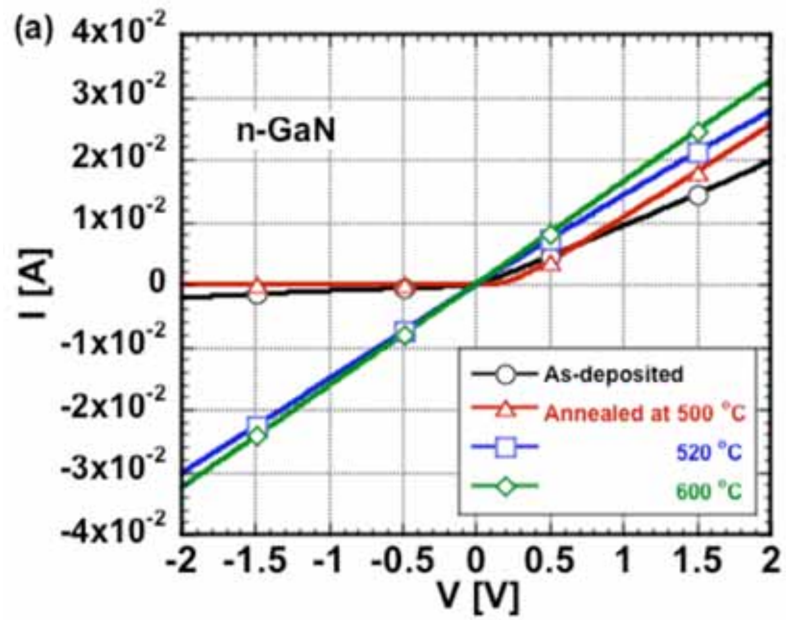

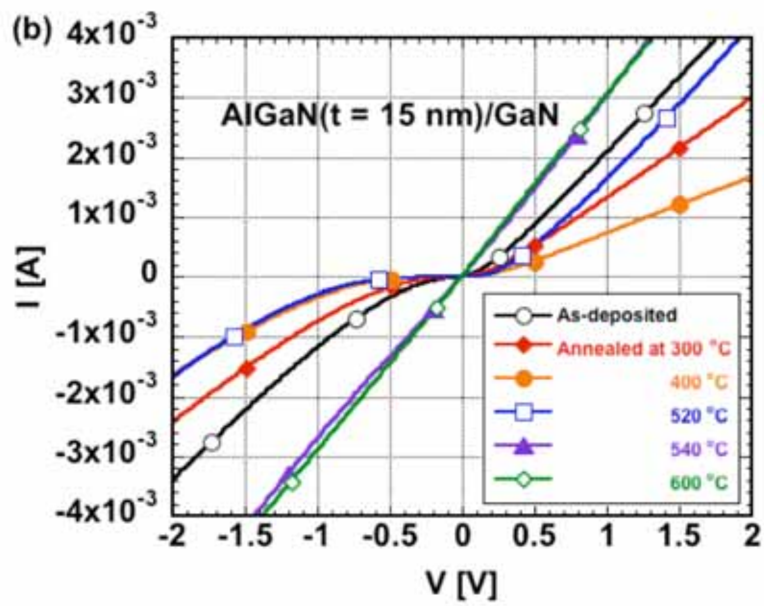

Fig. 2

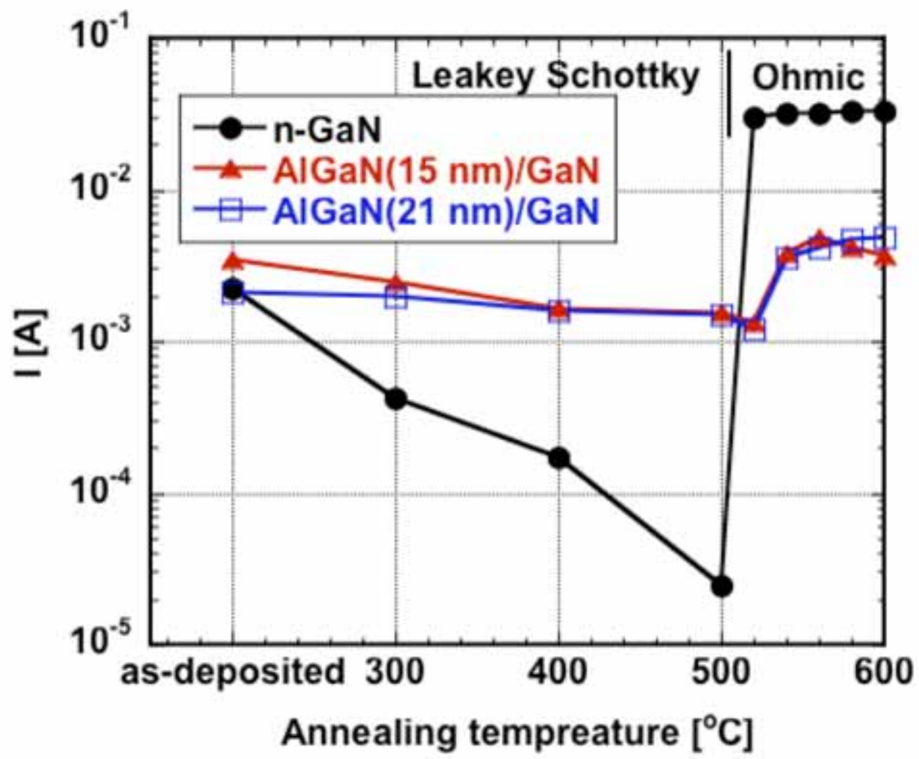

Fig. 3

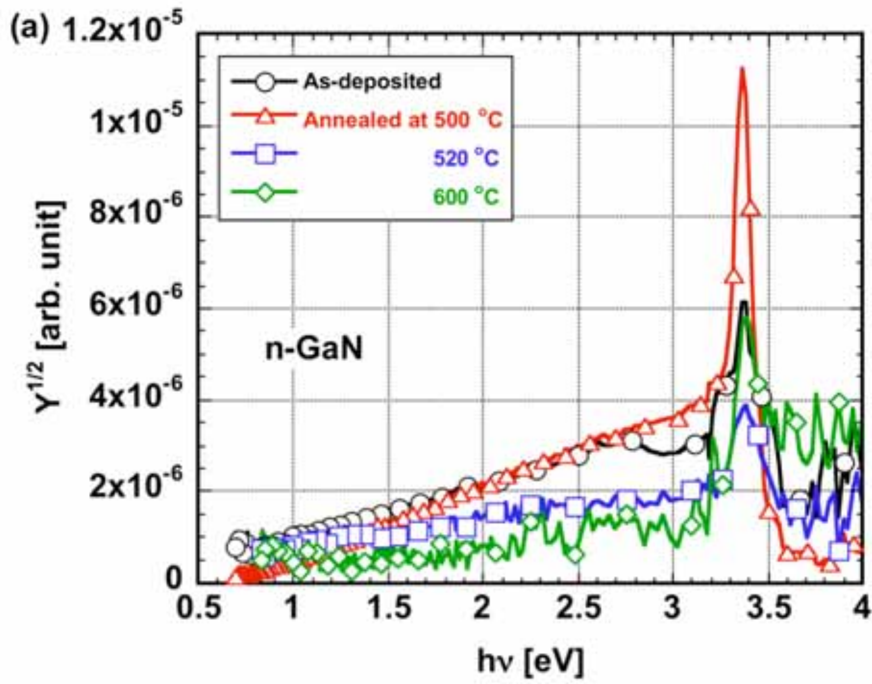

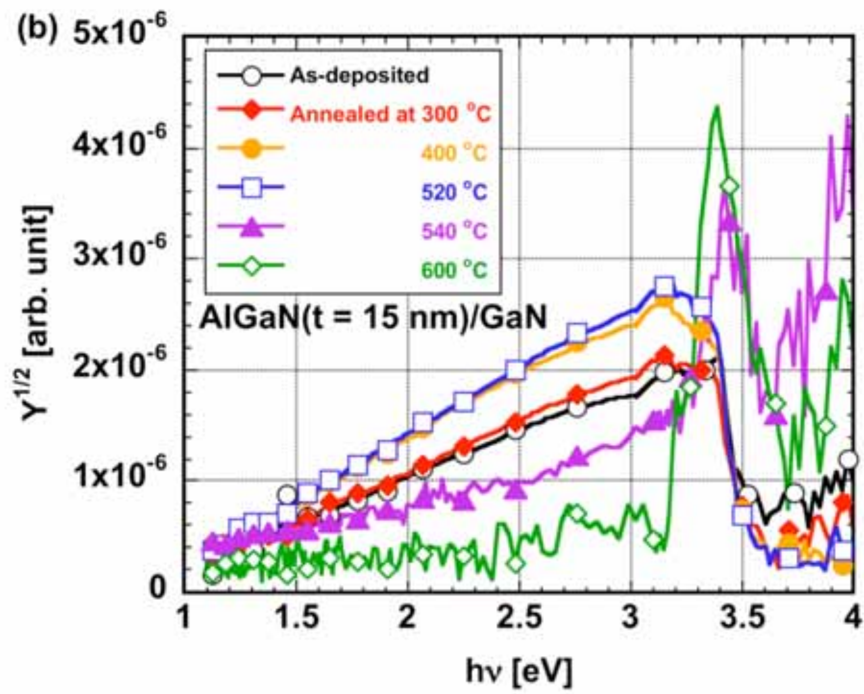

Fig. 4

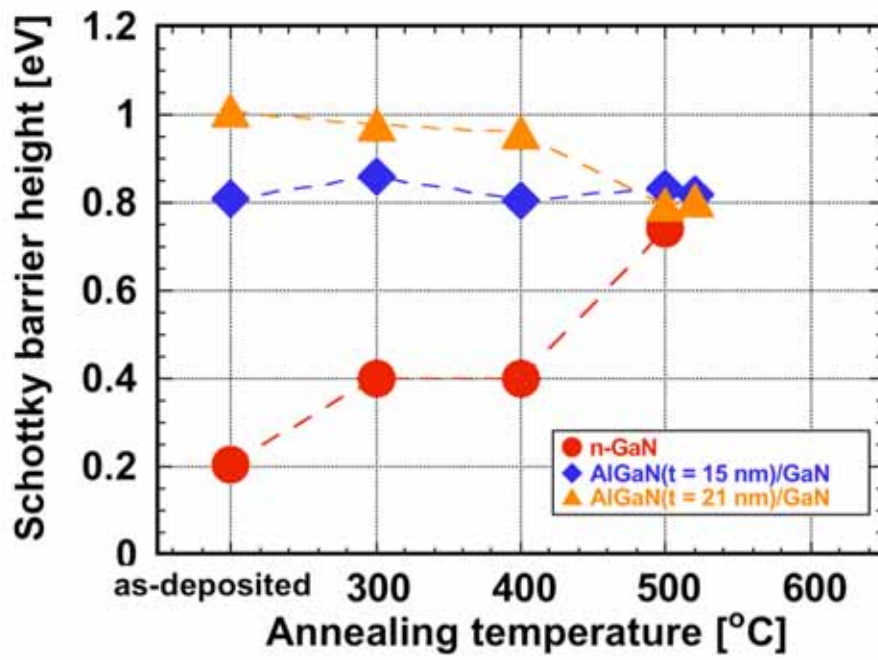

Fig. 5

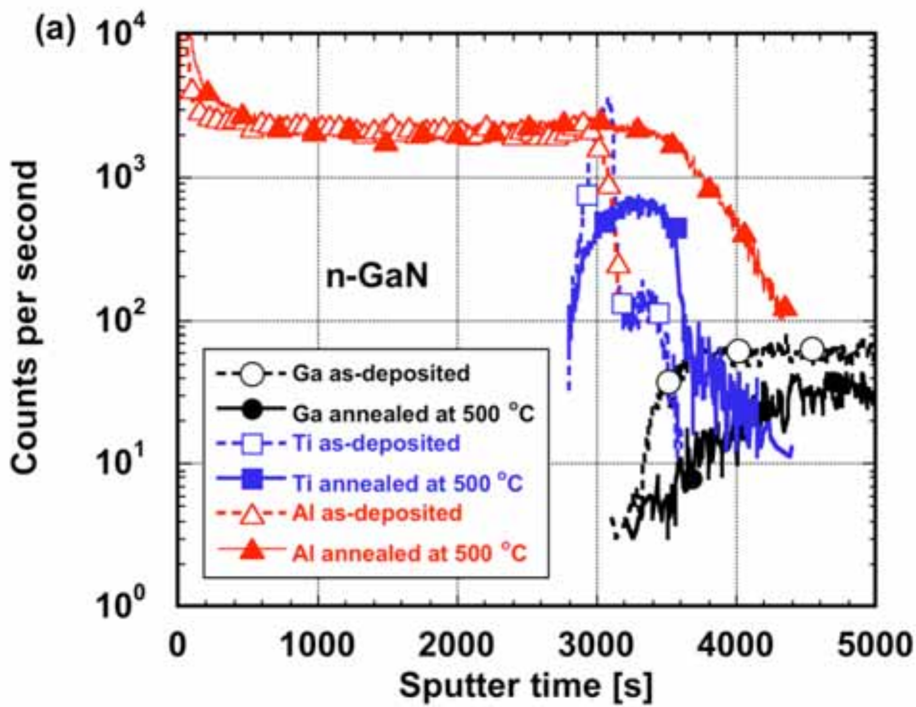

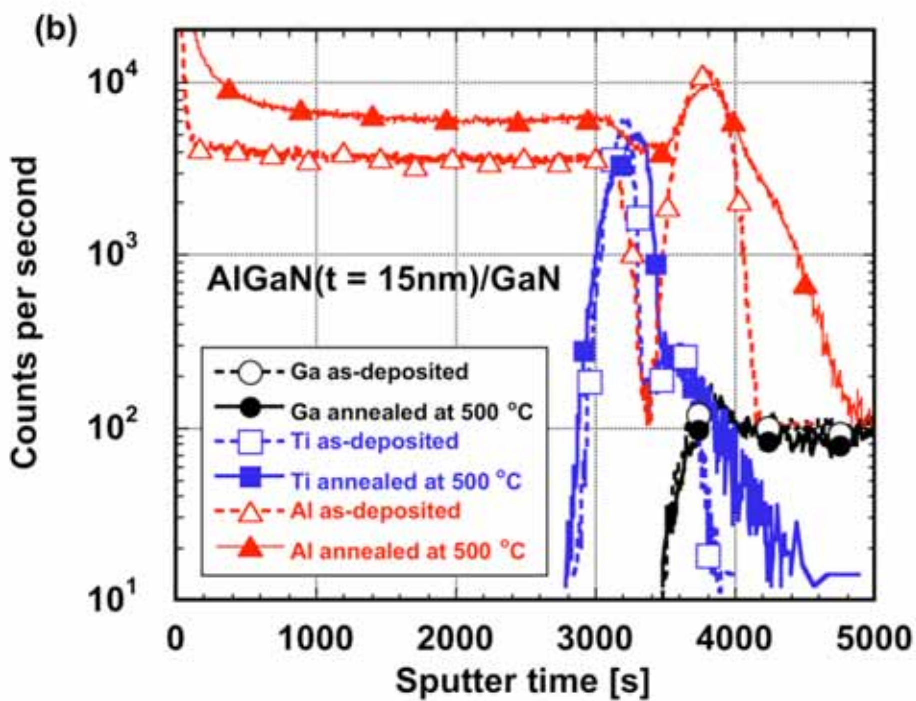

Fig. 6